Differential effects of subcutaneous and sublingual immunotherapy on timothy grass–specific T_H2 $CD4^+$ T-cell subsets

Hannah A. DeBerg, PhD,[a] Carolyn H. Baloh, MD,[b,c] Quinn DeGottardi, PhD,[d,e] Jue Hou, PhD,[d,f] Alexandra Johansson, MS,[d] Evan Newell, PhD,[f] Tanya M. Laidlaw, MD,[b,c] Srinath Sanda, MD,[b,g] Mohamed Shamji, PhD,[h] Stephen Durham, MD,[h] Alkis Togias, MD,[i] and William W. Kwok, PhD[d,j] *Seattle, Wash; Boston, Mass; San Francisco, Calif; London, United Kingdom; and Bethesda, Md*

Background: Allergen-specific $CD4^+$ T cells are a highly heterogenous population. Depletion of these cells has been proposed as essential to achieve allergen desensitization in allergen immunotherapy.

Objective: The overall aim of this study was to characterize the heterogeneity of timothy grass *(Phleum pratense)* allergen-specific $CD4^+$ T cells and determine how the frequency and phenotype of these cells change in response to sublingual (SLIT) and subcutaneous (SCIT) immunotherapy. Correlations between frequencies of these cells with Total Nasal Symptom Score and grass-specific serum immunoglobulin were also investigated.

Methods: Mass cytometry with lanthanides-tagged peptide major histocompatibility complex class II multimers and CD154 upregulation assays were used to examine changes in the frequency and phenotype of Phl p–specific $CD4^+$ T cells in longitudinal peripheral blood mononuclear cell samples from a randomized, double-blind, placebo-controlled trial of SLIT and SCIT. Supervised and unsupervised clustering was used for data analysis.

Results: Phenotypes of Phl p–specific T cells were highly heterogenous but could be categorized into two major metaclusters, $CRTH2^{hi}CD27^{lo}$ and $CRTH2^{lo}CD27^{hi}$, each with distinct phenotypic profiles. Weak positive correlations between Total Nasal Symptom Score and frequencies of T cells within both subsets were observed. SCIT preferentially depleted $CRTH2^{hi}CD27^{lo}$ cells, whereas SLIT depleted $CRTH2^{lo}CD27^{hi}$ cells. $CRTH2^{hi}CD27^{lo}$ cell frequency correlated with Phl p–specific IgE and IgG_4, but not IgA, levels.

Conclusion: Unsupervised clustering revealed distinct subpopulations of allergen-specific T cells that were differentially targeted and depleted by SCIT and SLIT, suggesting that SCIT and SLIT act through overlapping but distinct immunologic pathways. (J Allergy Clin Immunol 2026;■■■:■■■-■■■.)

Key words: *Allergic rhinitis, grass allergy, allergen immunotherapy, grass immunotherapy, antigen-specific T cells, grass-specific T cells, multimer positive T cells*

The prevalence of allergic rhinitis in adults is estimated to be 18% globally, with rates increasing over the past few decades.[1] Allergic rhinitis is a disease driven by type 2 inflammation; however, allergen-specific T_H1 cells are also observed.[2] Recent studies show that a special subset of T_H2 cells, with the phenotypic surface markers $CD161^+CD49d^+CRTH2^+CD27^-$, is uniquely present in people with allergic diseases. This subset of T_H2 cells, known as pathogenic T_H2A cells, is considered to be the main driver of pathogenic T_H2 responses in allergic individuals.[3-6]

Allergen immunotherapy has been used to retrain the immune system and induce tolerance for decades.[7] Subcutaneous immunotherapy (SCIT) needs to be administered for 3 to 5 years to obtain tolerance. While this therapy is generally recognized to be effective, the burden on patients is substantial because they have to receive the immunotherapy in a doctor's office.[8] As a result, sublingual immunotherapy (SLIT) was developed to try to reduce the burden by allowing at-home dosing.[9]

The GRASS (Long-Term Effects of Sublingual Grass Therapy) clinical trial was performed to determine whether a shorter duration of therapy with SLIT could induce tolerance.[10] The GRASS trial was a single-site, randomized, placebo-controlled, 3-arm study comparing timothy grass SCIT, timothy grass SLIT, and placebo for the treatment of grass allergy. One hundred six adults with timothy grass *(Phleum pratense)* allergy were randomized to treatment with SCIT, SLIT, or placebo for 2 years, followed by 1 year off therapy. By the end of 2 years of therapy, the Total Nasal Symptom Score (TNSS) (weighted 10-hour area under the curve) during a nasal allergen challenge was significantly lower in both the SCIT and SLIT arms compared to placebo. After 1 year off therapy, the TNSS (10-hour area under the curve) returned toward baseline and was not significantly different between the 3 trial arms.

From [a]the Center for Systems Immunology, Benaroya Research Institute (BRI) at Virginia Mason, Seattle; [b]the Immune Tolerance Network, BRI at Virginia Mason, Seattle; [c]the Division of Allergy and Clinical Immunology, Brigham and Women's Hospital, and Harvard Medical School, Boston; [d]the Center for Translational Immunology, BRI at Virginia Mason, Seattle; [e]the Seattle Children's Research Institute, Seattle; [f]the Vaccine and Infectious Disease Division, Fred Hutchinson Cancer Center, Seattle; [g]the Division of Endocrinology, UCSF Diabetes Center, UCSF School of Medicine, University of California, San Francisco; [h]the Immunomodulation and Tolerance Group, Allergy and Clinical Immunology, Department of National Heart and Lung Institute, London; [i]The National Institute of Allergy and Infectious Disease, Bethesda; and [j]the Division of Allergy and Infectious Disease, Department of Medicine, University of Washington, Seattle.

The first 4 authors contributed equally to this article, and all should be considered first author.

Received for publication October 21, 2025; revised January 27, 2026; accepted for publication February 18, 2026.

Corresponding author: William W. Kwok PhD, Benaroya Research Institute, 1201 Ninth Ave, Seattle, WA 98101. E-mail: bkwok@benaroyaresearch.org.

0091-6749/$36.00

https://doi.org/10.1016/j.jaci.2026.02.026

Abbreviations used
CyTOF: Cytometry by time of flight
ddH_2O: Double-distilled H_2O
PBMC: Peripheral blood mononuclear cell
PE: Phycoerythrin
RT: Room temperature
SCIT: Subcutaneous immunotherapy
SLIT: Sublingual immunotherapy
TNSS: Total Nasal Symptom Score
UMAP: Uniform manifold approximation and projection

Several biomarkers, including grass-specific IgG_4-to-IgE ratio, percentage of allergen-IgE complexes binding to B cells *in vitro,* and basophil activation, correlated with clinical response patterns.[11] At year 2 of this study, a significant sustained reduction in circulatory T_H2A cells was observed only in the SCIT arm and not in the SLIT arm, even though both treatment arms similarly improved in the primary outcome of TNSS during nasal allergen challenge.[11] Given the heterogeneity of $CD4^+$ T cells, these previous findings raise the possibility that depletion of subsets of T_H2 cells other than T_H2A cells may be critical for attaining desensitization with the SLIT group. To explore this, we used a panel of 25 antibodies, multiple peptide major histocompatibility complex (MHC) class II multimers and CD154 upregulation assays in mass cytometry experiments to analyze frequencies, surface phenotypes, and cytokine profiles of Phl p–specific $CD4^+$ T cells during the course of immunotherapy. These data were then analyzed in both supervised and unsupervised approaches. The results confirmed that T_H2 cells are highly heterogenous. We further examined how immunotherapy affects these different T-cell subsets, how these different T_H2 cell subsets are related to one another, and how they influence TNSS and antibody responses.

METHODS

Sample and clinical data collection

Peripheral blood mononuclear cells (PBMCs) were collected from GRASS trial participants at baseline; after 1 and 2 years of SCIT, SLIT, or placebo; and after 1 year off therapy. PBMCs were cryopreserved as previously described.[10] Clinical data corresponding to the samples were obtained from the Immune Tolerance Network's TrialShare website (itntrialshare.org).

Multimer production and assembly

Myc-tagged HLA-II monomer reagents were produced from S2 cells transfected with HLA-II complementary DNA as previously described.[12] In brief, transfected S2 cells were expanded to a 2 L volume in spinner flasks (Bellco, Vineland, NJ) and induced for 5 days with 1 mmol copper sulfate, adding 2 μg/mL biotin to ensure efficient protein biotinylation. Supernatants were separated from intact cells by centrifugation (11,000*g*), separated from debris with a 0.2 μm filter (Thermo Fisher Scientific, Waltham, Mass), and then affinity purified with L243 coupled with CNBr-Activated Sepharose 4B (GE Healthcare, Pittsburgh, Pa). Class II protein was eluted at pH 11.5, equilibrated with pH 4.0 Tris buffer, and exchanged into a pH 6.0 storage buffer (0.2 mol sodium phosphate). Phl p–specific $CD4^+$ T-cell epitopes were identified by Tetramer Guided Epitope Mapping, as described elsewhere.[11] Class II monomers were loaded with individual peptides by incubating for 72 hours at 37°C in the presence of 2.5 mg/mL *n*-octyl-β-d-glucopyranoside (Sigma, St Louis, Mo). Multimers were formed by individually incubating class II molecules with metal-labeled streptavidin or phycoerythrin (PE)-labeled streptavidin (Thermo Fisher Scientific) for 6 to 18 hours at room temperature (RT) at a molar ratio of 8:1. Metal-labeled streptavidin was produced as previously described.[13,14] Multimers used in this study are listed in Table E1 in this article's Online Repository available at www.jacionline.org.

Multimer-based immune cell profiling via mass cytometry

Approximately 20 million frozen PBMCs were thawed and subjected to multimer staining. Initially, cells were resuspended in 200 μL of T Cell Medium, which consists of RPMI 1640, 10% human serum, L-glutamine, HEPES buffer, and sodium pyruvate. Subsequently, dasatinib (Santa Cruz Biotechnology, Santa Cruz, Calif) was added to the cell suspension at a final concentration of 50 nmol. This mixture was incubated at 37°C for 5 minutes. Next, 3 μL (500 μg/mL) of each metal-tagged multimer was added. The cells were incubated at RT for 2 hours, with intermittent stirring every 30 minutes. After the incubation period, cells were washed with 3 mL of running buffer (1× PBS, EDTA, sodium azide), then resuspended in 175 μL of running buffer plus 25 μL of anti–c-Myc microbeads (Miltenyi Biotec, San Diego, Calif) for 15 minutes at 4°C. The cells were washed and resuspended in 1 mL of running buffer, and a 20 μL fraction was retained. The multimer-positive cells were enriched through a mass spectrometry column (Miltenyi Biotec) following the manufacturer's instructions. The enriched cells, alongside the preenrichment fraction, were stained with an extracellular antibody cocktail that consisted of 25 antibodies (see Table E2 in the Online Repository available at www.jacionline.org) for 25 minutes at RT. Cisplatin was added (final concentration 25 μmol) at 24 minutes, immediately followed by quenching with 3 mL of running buffer. Cells were washed with 1× PBS and resuspended in 500 μL 1× PBS with iridium (125 nmol), then incubated for 30 minutes at RT. Cells were washed with 1× PBS, spun down, and resuspended in 150 μL IC Fixation Buffer (eBioscience; Thermo Fisher Scientific) and incubated at RT for 45 minutes. Cells were then washed once with 1× PBS and twice in double-distilled H_2O (ddH_2O). Finally, the cells were resuspended in ddH_2O, spiked with EQ beads (Fluidigm, San Francisco, Calif), and immediately analyzed via cytometry by time of flight (CyTOF). Data normalization was performed using EQ beads and CyTOF v2 software, and FCS files were analyzed by FlowJo software (Becton Dickinson, Franklin Lakes, NJ). For the multimer analysis, cells positive for each specific multimer-labeled lanthanide were individually gated (see Fig E1 in the Online Repository) and Boolean gated to identify multimer-specific T cells. The frequency of epitope-specific cells was calculated using the following formula: F = [1,000,000 × (multimer positive events from enriched tube/10× number of $CD4^+$ T cells from the "pre" fraction)].

CD154 upregulation assay and intracellular cytokine staining of timothy grass–specific CD4$^+$ T cells

Twenty million frozen PBMCs were thawed, rested for 4 hours at RT, and incubated *in vitro* for 16 hours with timothy grass peptide libraries from Phl p 1, Phl p 5a, and Phl p 5b. Peptides were 20 aa in length with a 12 aa overlap (mimotopes). Each peptide was used at a final concentration of 0.5 μg/mL. Anti-CD40 antibody (1 μg/mL, Miltenyi Biotec) was also added to inhibit the downregulation of CD154, preventing CD40/CD154 interactions on newly activated T cells. After stimulation, the PBMCs were stained with anti–CD154-PE antibody (Miltenyi Biotec) for 30 minutes at RT. Cells were then incubated with anti-PE beads, and the CD154$^+$ cells were enriched through a Miltenyi Biotec mass spectrometry column. Cells were washed and stained with anti-PE metal conjugate as well as a panel of cell surface antibodies that included anti-CD69, anti-CD27, and anti-CRTH2 (see Table E3 in the Online Repository available at www.jacionline.org). The cells underwent a 30-minute incubation at RT. In the final minute of incubation, cisplatin was added to the sample and then quickly quenched with 3 mL of running buffer. The cells were washed with 1× PBS, resuspended in 500 μL of 1× PBS containing iridium, and incubated for another 30 minutes at RT.

Next the cells were fixed with 150 μL of IC Fixation Buffer (eBioscience) and incubated at RT for 45 minutes. This was followed by a 30-minute permeabilization step using Permeabilization Buffer (eBioscience). The cells were then stained with an intracellular cytokine antibody cocktail, including GM-CSF, IFN-γ, IL-4, IL-5, IL-9, IL-10, IL-13, IL-17A, IL-21, and TGF-β (Table E3) at pretitrated concentration and incubated for 30 minutes at RT. After washing with 1× permeabilization buffer and 1× PBS, followed by two rinses in ddH_2O, cells were resuspended in ddH_2O. EQ beads (Fluidigm) were then added, and the cells were immediately analyzed on the CyTOF machine. Analysis of the flow cytometry standard (FCS) files was conducted by FlowJo software. Antigen-responsive T cells were identified on the basis of the upregulation of both CD154 and CD69 on CD4$^+$ T cells.

Mass cytometry data analysis

FCS files were analyzed by R software (www.r-project.org). Files were read into R with the 'flowCore' package.[15] Marker intensities were transformed using an inverse hyperbolic sine transformation (arcsinh) with parameters $a = 0$, $b = 0.2$. To adjust for batch differences between samples, z score normalization was applied to each marker relative to the total CD4$^+$ T-cell expression for that marker on the same subject and visit before dimensionality reduction. Dimensionality reduction was performed by the uniform manifold approximation and projection (UMAP) algorithm as implemented in the UMAP R package. Normalized event profiles were clustered by the PhenoGraph algorithm, as implemented in the R Phenograph package, and visualized by ComplexHeatmap. For plotting frequencies, a pseudocount of 1 cell per million was added to allow use of a log scale for visualization purposes. The 'learn_graph()' function from the R package Monocle was used to construct a trajectory.[16]

Statistics

ANOVA was used to compare TNSS, timothy grass IgE, and timothy grass IgG_4 across treatment groups at baseline. A chi-square test was used to compare the effect of biological sex across treatment groups. Cell frequencies were compared by Wilcoxon rank sum test with a false discovery rate multiple testing correction. The linear Pearson correlation coefficient was used to evaluate TNSS and timothy grass–specific T-cell frequencies, and Spearman rank–based correlations were used to examine timothy grass–specific IgE, IgG_4, and IgA_1 as well as timothy grass–specific T-cell frequencies.

RESULTS

Forty-four participants from the GRASS study were included in this project (n = 13 placebo, n = 14 SCIT, n = 17 SLIT). Table I summarizes the demographics and baseline clinical measures of these participants. There were no statistically significant differences in age, sex balance, TNSS, timothy grass–specific IgE, or timothy grass–specific IgG_4 at baseline.

Using lanthanide Phl p–specific multimers and a panel of 25 different antibodies, the frequency and phenotype of Phl p–specific CD4$^+$ T cells was characterized before treatment with allergen immunotherapy (baseline); during treatment at the end of years 1 and 2; and 1 year after stopping treatment (year 3). As a control, rhinovirus-specific CD4$^+$ T cells were examined in parallel. Fig 1 shows DR0101 multimer staining results for one DR0101 participant. At baseline, Phl p 1–specific T cells were CCR4$^+$CRTH2$^+$CD27$^-$—phenotypic properties of T_H2A cells. Compared to the placebo group, the frequency of Phl p–specific CD4$^+$ T cells was significantly decreased at years 1 and 2 of treatment in the SLIT group, and this decrease was still observed between the SLIT group and placebo at year 3 after 1 year of no treatment (Fig 2, *A*). In contrast, the frequency of rhinovirus-specific CD4$^+$ T cells for all 3 groups remained unchanged throughout the study (Fig 2, *B*). Standard biaxial gating that used CRTH2 as a marker for T_H2A cells also revealed a significant decrease in the frequency of Phl p–specific CD4$^+$ T cells in both the SLIT and SCIT groups at year 1 compared to placebo, furthermore this decrease was only observed in the SCIT group at years 2 and 3 (Fig 2, *C*). There was no significant difference in T_H2A frequencies between the SLIT and SCIT groups.

Unsupervised clustering was used to further characterize the phenotype of Phl p–specific CD4$^+$ T cells. Data visualization via UMAP with Phenograph clustering with Phl p–specific cells from all 4 time points identified Phl p–specific CD4$^+$ T cells segregating into 8 distinct clusters (Fig 3, *A*), which were further categorized into 2 metaclusters: a CRTH2^{hi}CD27^{lo} metacluster including clusters 4-8, and a CRTH2^{lo}CD27^{hi} metacluster including clusters 1-3 (Fig 3, *B* and *C*, and see Fig E2 in the Online Repository available at www.jacionline.org). Cells within the CRTH2^{hi}CD27^{lo} metacluster were characterized by high expression of CRTH2 and CD49d, and low expression of CD27, consistent with the T_H2A cell phenotype (Fig 3, *D*, Fig E2). Within the CRTH2^{hi}CD27^{lo} metacluster, clusters 4 and 5 exhibited all the hallmarks of the T_H2A subset (CRTH2$^+$CD49d$^+$CD161$^+$CD27$^-$) but were distinguished by CD39 expression. Compared to the other clusters in this metacluster, cluster 4 cells expressed the highest levels of CD49d, CD161, and inducible T-cell costimulator; cluster 6 cells expressed the lowest levels of CD161; cluster 7 had the lowest expression of CD25 and CD127; and cluster 8 cells had very low CCR4 expression. Within the CRTH2^{lo}CD27^{hi} metacluster, cluster 2 expressed CXCR3 whereas clusters 1 and 3 were CCR4$^+$ and CXCR3$^-$,

TABLE I. Demographic and baseline clinical characteristics of study participants

Treatment	No. of participants with: DR0101	DR0301	DR0401	DR0701	DR1101	Total no. of participants	Median age (years)	Sex, M/F	TNSS score	Baseline mean (SD) of: TG IgE (kU_A/L)	TG IgG_4 (kU_A/L)
Placebo	4	4	6	5	2	13	29.4	9/4	6.33 (2.29)	56.14 (48.06)	0.29 (0.26)
SCIT	6	4	1	5	1	14	27.4	8/6	6.53 (2.14)	36.28 (38.16)	0.32 (0.18)
SLIT	3	4	5	9	1	17	35	14/3	5.66 (1.74)	53.62 (89.63)	0.41 (0.4)

TG, Timothy grass.

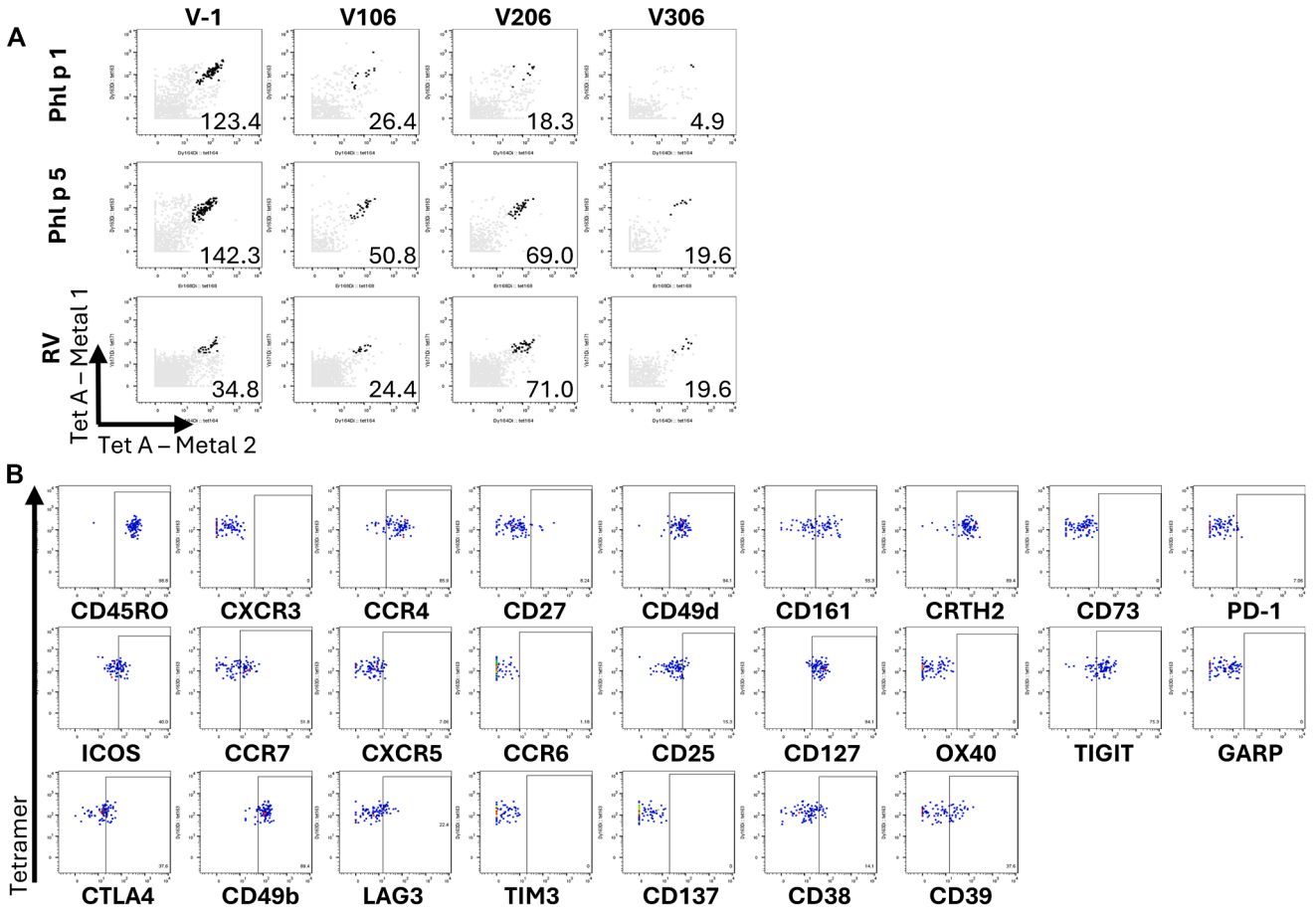

FIG 1. *Ex vivo* class II multimer staining. **(A)** Combinatorial *ex vivo* class II multimer staining of Phl p 1–specific, Phl p 5–specific, and rhinovirus (RV)-specific $CD4^+$ T cells at 4 different time points. Combinatorial multimer staining was carried out in PBMCs from DR0101 subject at baseline and years 1, 2, and 3 after treatment. Multimer for each epitope specificity was conjugated to 2 different metal tags, as shown in Table E1. Staining for specific T cells of different epitope specificities at each time point was carried out in single tube. *Dark dots* represent epitope-specific $CD4^+$ T cells; *gray dots,* other $CD4^+$ T cells. Frequencies of epitope-specific $CD4^+$ T cells per million $CD4^+$ T cells are indicated. Gating strategy for identification of multimer positive T cells is shown in Fig E1. **(B)** Phenotypic cell surface markers of gated DR0101/Phl p 1–specific T cells at baseline.

markers characteristic of conventional T_H2 cells, but had distinct expression profiles for CD161, CD49d and CD25. Cells in $CRTH2^{lo}CD27^{hi}$ metacluster also expressed lower levels of TIGIT, CTLA-4, and CD39 compared to the $CRTH2^{hi}CD27^{lo}$ metacluster. Pseudotime trajectory was also used to infer the relationship between these different subsets of T cells. A transition of cells from cluster 1 to cluster 5 was observed (see Fig E3 in the Online Repository).

The frequency of cells within each metacluster in response to SCIT and SLIT was also examined. Compared to the placebo group, the frequency of the $CRTH2^{hi}CD27^{lo}$ metacluster decreased in response to SCIT but not SLIT, and this persisted

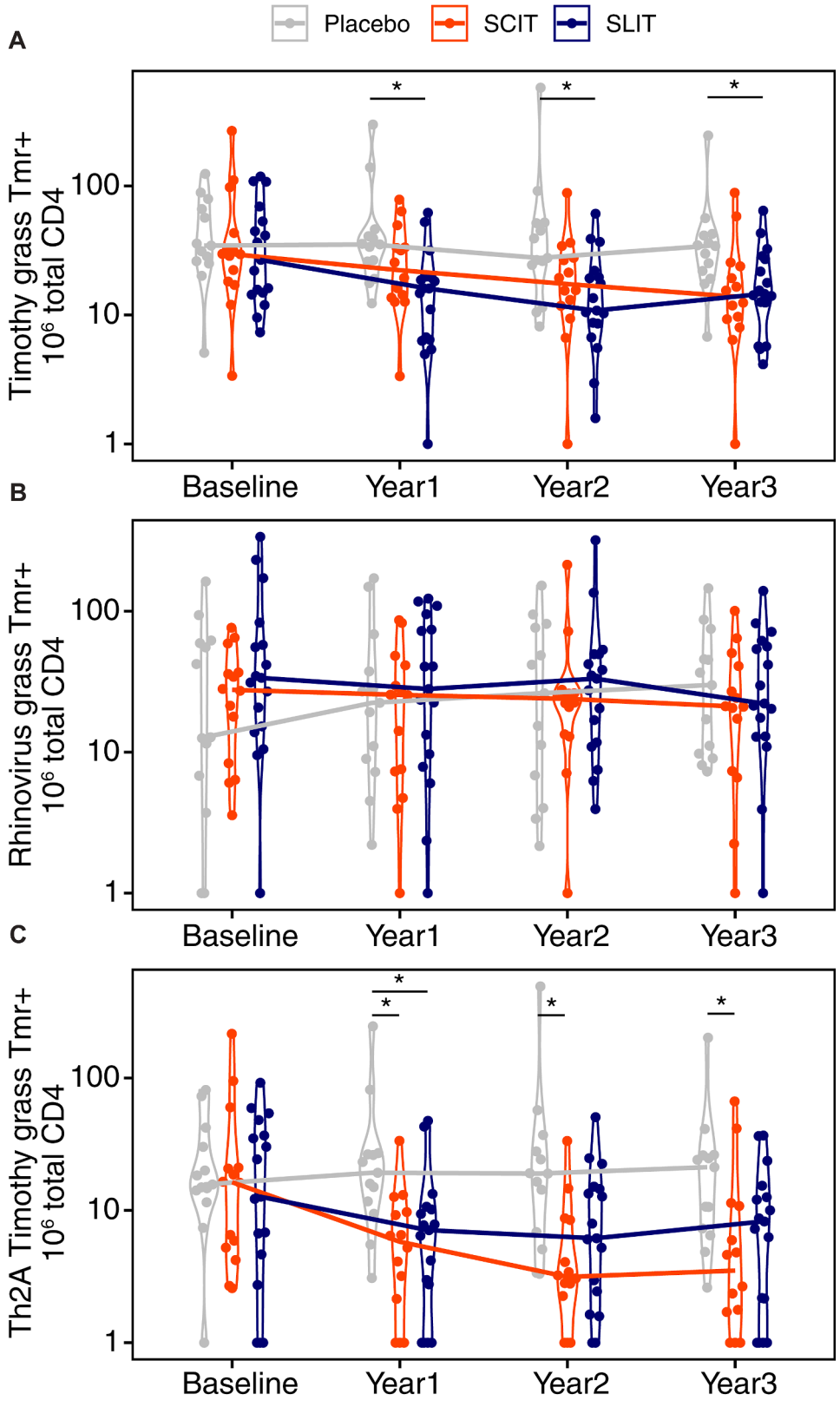

FIG 2. Frequencies of timothy grass–specific and rhinovirus (RV)-specific T cells as determined by tetramer staining throughout courses of study. **(A)** Summed frequencies of timothy grass–specific T cells. Each data point represents summed total frequencies of all timothy grass–specific T cells from 1 subject. **(B)** Frequencies of RV-specific T cells. **(C)** Frequencies of timothy grass–specific T cells with T_H2A phenotype. *Points* show individual frequencies; *lines* connect medians.

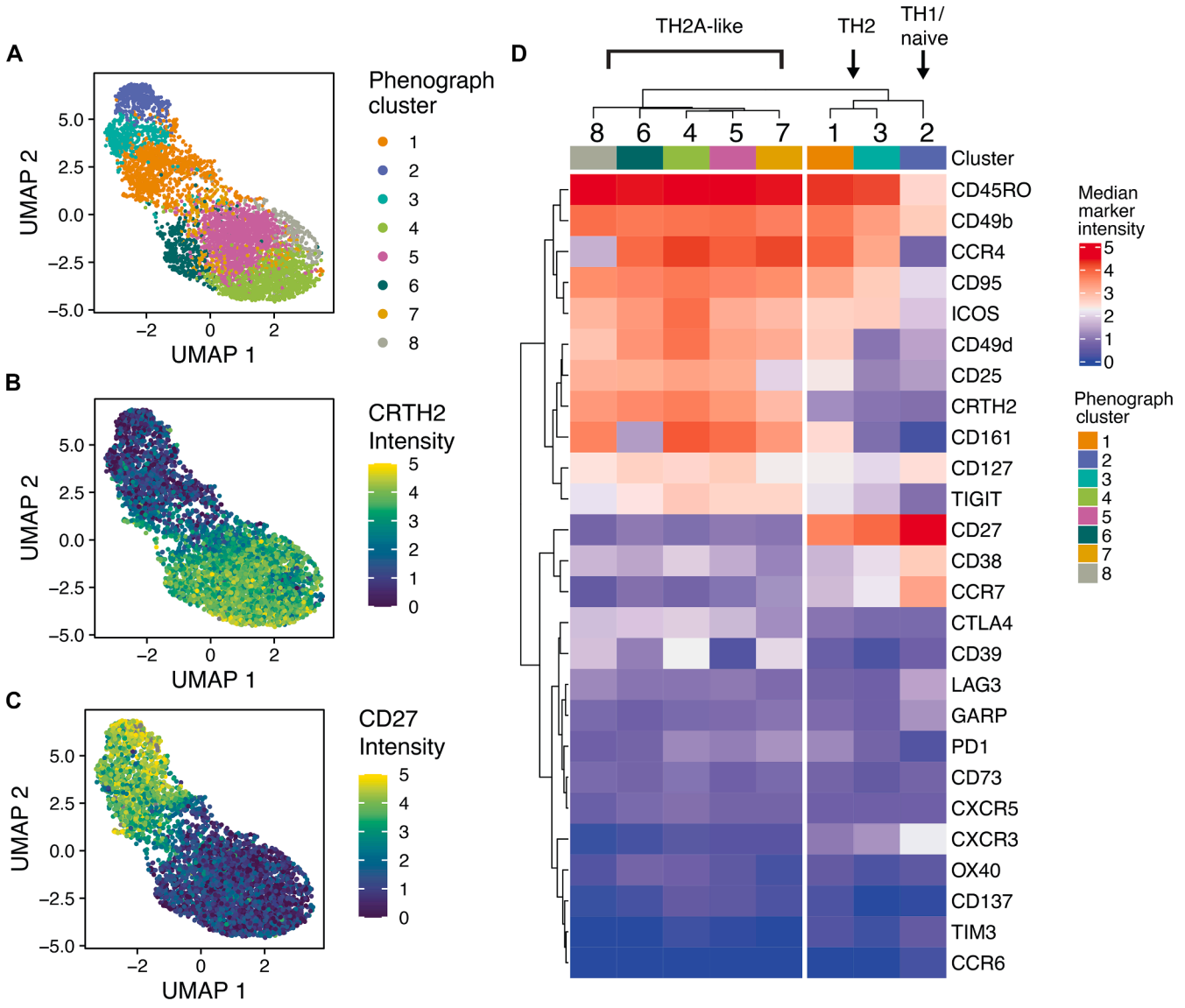

FIG 3. Cellular clustering of timothy grass–specific T cells with multimer staining assays. **(A)** UMAP dimensionality reduction and PhenoGraph clustering were applied for CyTOF data set for examination of surface markers of timothy grass–specific T cells. Total of 5,375 cells were examined. We identified 8 clusters of timothy grass–specific T cells. (**B** and **C**) Eight clusters of T cells were grouped into 2 major metaclusters as defined by CRTH2 and CD27 surface expression. **(D)** Cell surface marker expression of different timothy grass–specific T-cell subsets.

to year 3 (Fig 4, *A*). In contrast, the frequency of the CRTH2^{lo}CD27^{hi} metacluster decreased in response to SLIT but not SCIT (Fig 4, *B*). Examination of the individual clusters comprising the metaclusters indicated that cluster 5 is predominantly the driver of metacluster CRTH2^{hi}CD27^{lo} response to therapy in year 2, whereas cluster 3 is the driver of metacluster CRTH2^{lo}CD27^{hi} response in year 1 (see Fig E4 in the Online Repository available at www.jacionline.org).

The distributions of Phl p 1, Phl p 5a, and Phl p 5b within two major metaclusters were examined. There were significantly more Phl p 1–specific CD4^{+} T cells in the CRTH2^{hi}CD27^{lo} metacluster and more Phl p 5b–specific CD4^{+} T cells in the CRTH2^{lo}CD27^{hi} metacluster (Fig 4, *C*). However, because of the small numbers of cells analyzed, we were unable to clearly assess differences in grass component–specific T cells over time.

To further characterize the functional differences between the two metaclusters, additional PBMC samples were obtained from the current cohort, and CD154 upregulation assays were carried out for cytokine analysis. CD154^{+}CD69^{+} cells were defined as timothy grass–specific CD4^{+} T cells in these assays. Unsupervised clustering of these antigen-reactive cells subdivided these cells into 13 different clusters, which were further classified into two major populations corresponding to CRTH2^{hi}CD27^{lo} and CRTH2^{lo}CD27^{hi} phenotypes (Fig 5, *A* and *B*). We noted that CRTH2^{hi} cells expressed a higher level of CD154 compared

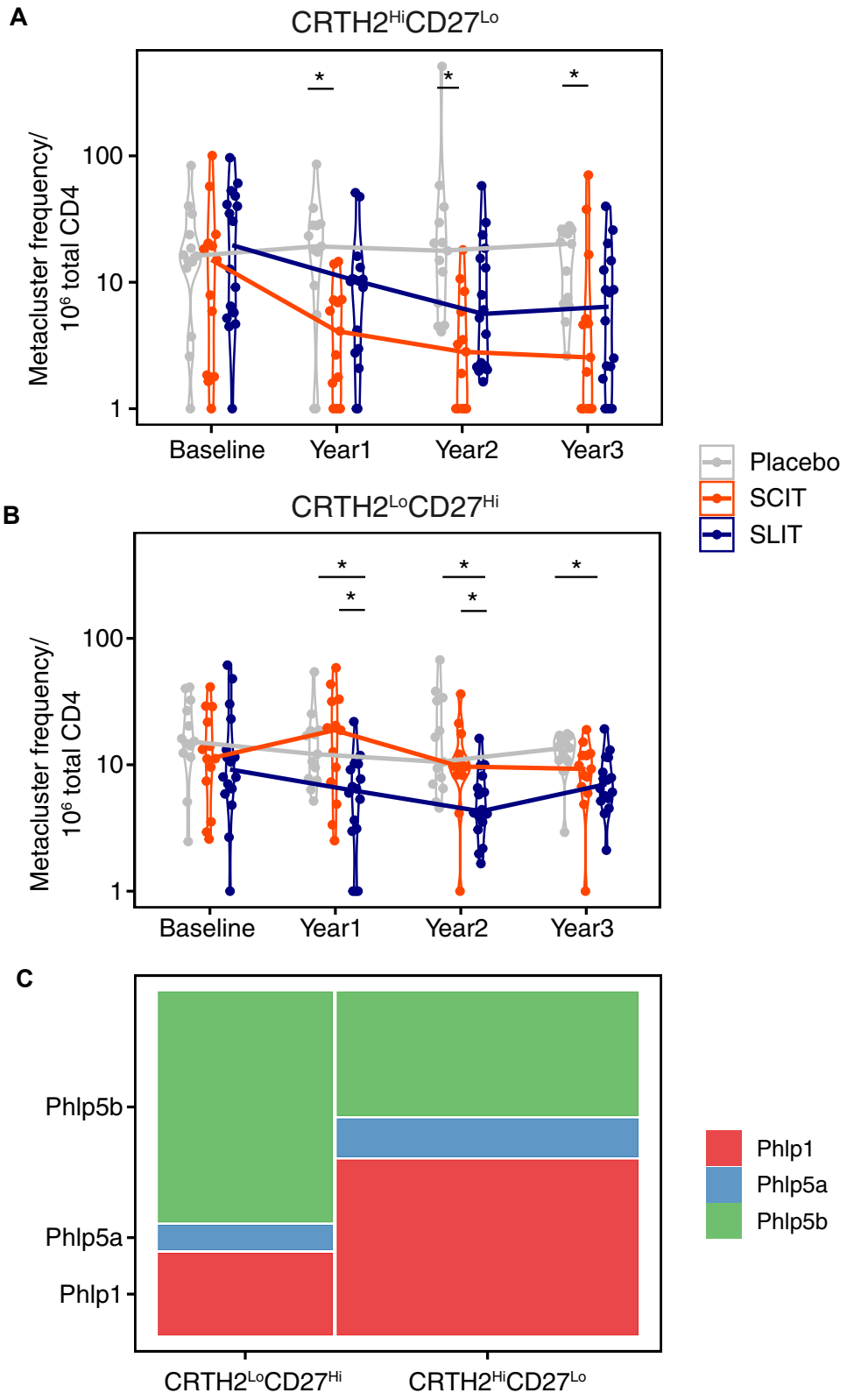

FIG 4. Phl p–specific $CD4^+$ T cells in $CRTH2^{hi}CD27^{lo}$ and $CRTH2^{lo}CD27^{hi}$ subsets. (**A** and **B**) Differential decline of timothy grass–specific $CD4^+$ T cells in $CRTH2^{hi}CD27^{lo}$ and $CRTH2^{lo}CD27^{hi}$ subsets during SCIT and SLIT treatment. *Points* show individual frequencies; *lines* connect medians. **(C)** Mosaic plot with rectangle areas proportional to numbers of Phl p 1–, Phl p 5a–, and Phl p 5b–specific T cells in $CRTH2^{hi}CD27^{lo}$ and $CRTH2^{lo}CD27^{hi}$ subsets.

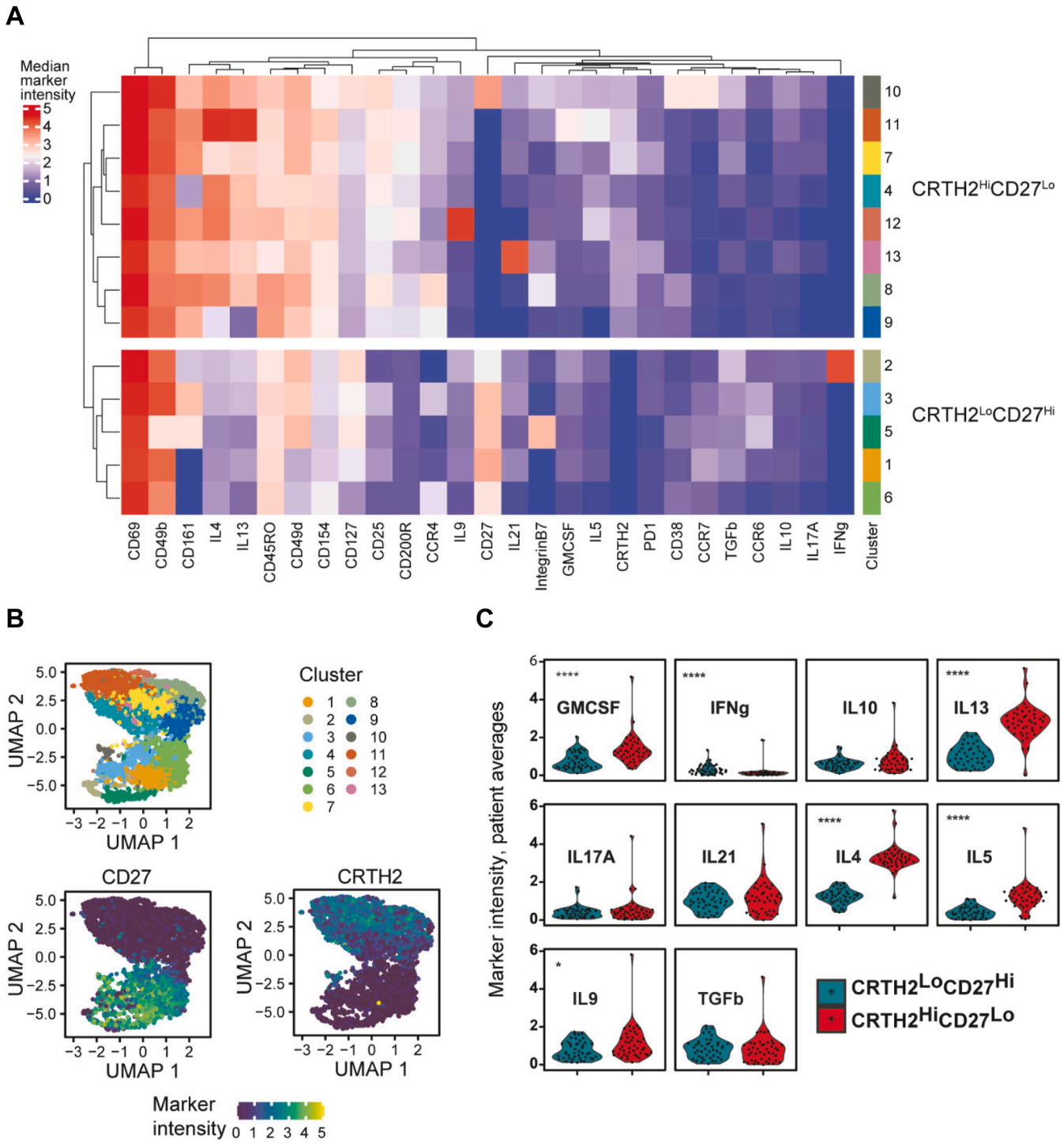

FIG 5. Cellular clustering of timothy grass–specific T cells with CD154 upregulation assays. **(A)** Total of 5,063 timothy grass–specific cells, as defined by $CD154^{+}CD69^{+}$ T cells, were examined. Unsupervised clustering led to identification of 13 clusters. **(B)** UMAP display of 13 different clusters, which were subdivided into 2 major metaclusters. **(C)** Cytokine profiles of $CRTH2^{hi}CD27^{lo}$ and $CRTH2^{lo}CD27^{hi}$ clusters.

to $CRTH2^{lo}$ cells (Fig 5, *A*), implying that $CRTH2^{hi}$ cells have a lower threshold of activation compared to $CRTH2^{lo}$ cells. The $CRTH2^{hi}$ cluster has significantly higher levels of GM-CSF, IL-4, IL-5, IL-9, and IL-13, whereas the $CRTH2^{lo}$ cluster exhibited significantly higher levels of IFN-γ (Fig 5, *C*).

Previous studies of the parent cohort for the current investigation demonstrated that both SCIT and SLIT significantly reduced TNSS compared to the placebo group at year 2.[10] The current cohort, comprising approximately a third of the parent cohort (44 vs 102 enrollees), exhibited a similar trend (Fig 6, *A*). Weak

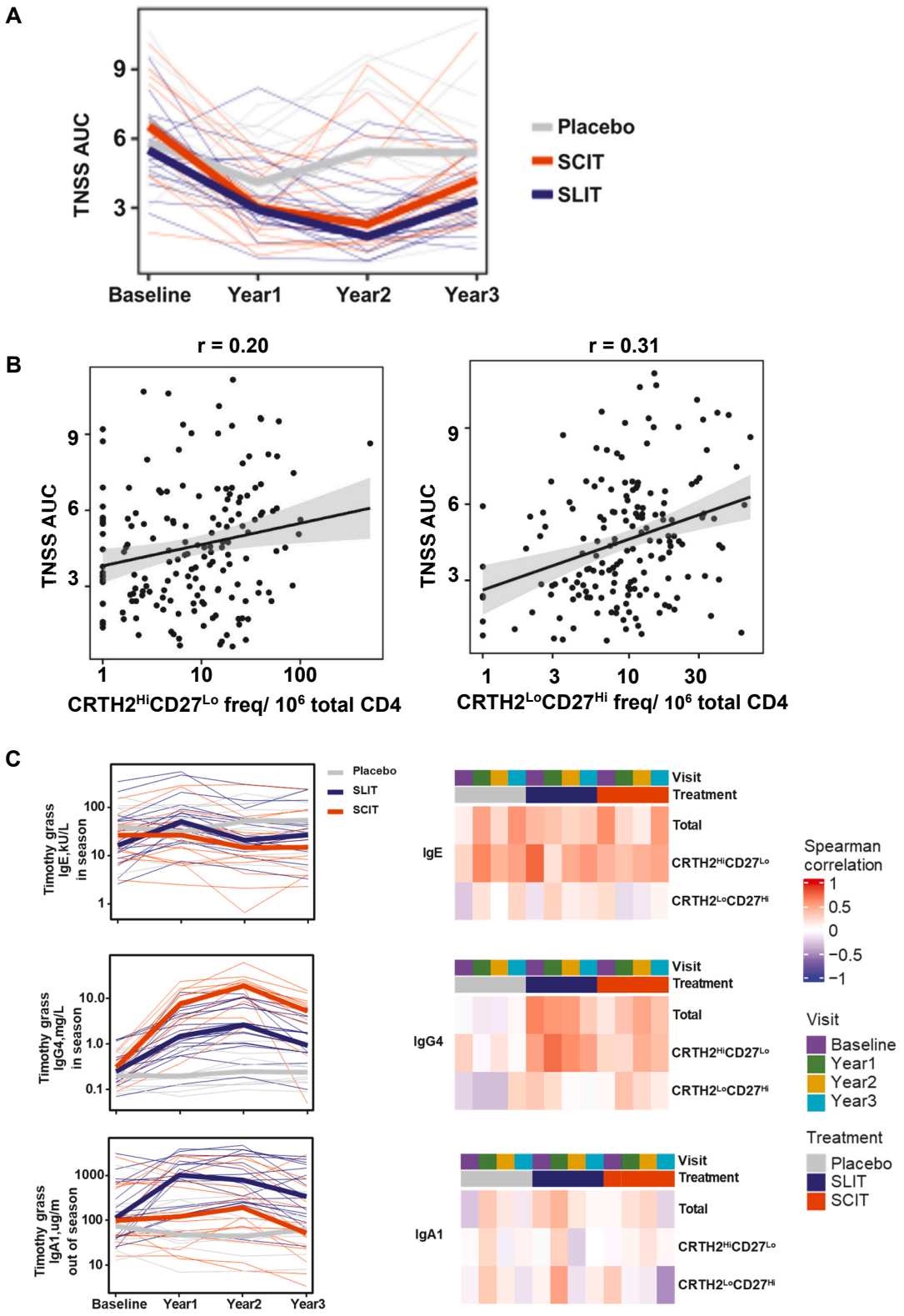

FIG 6. Correlation between TNSS, serum timothy grass–specific immunoglobulin levels, and frequency of different Phl p-specific T-cell subset. **(A)** TNSS average area under curve (AUC) for 0 to 10 hours after nasal challenge. **(B)** Pearson linear correlation between frequencies of allergen-specific $CD4^+$ T cells as measured by class II multimers and TNSS score. Pearson correlation coefficients are shown above plots. **(C)** Serum timothy grass–specific IgE, IgG_4, and IgA_1 level during immunotherapy. *Thin lines* show individual donors; *thick lines* indicate medians. **(D)** Spearman correlation between IgE, IgG_4, and IgA_1 levels and frequency of total, $CRTH2^{hi}CD27^{lo}$, and $CRTH2^{lo}CD27^{hi}$ Phl p–specific $CD4^+$ T cells.

positive correlations were observed between the frequencies of T cells in both metaclusters and TNSS scores (Fig 6, *B*). These modest correlations underscore the contribution of tissue-resident immune responses and humoral mechanisms, beyond peripheral allergen-specific T-cell frequencies, to clinical symptom severity as reflected by TNSS.

While the timothy grass–specific IgE level remained fairly flat throughout the course of the study, timothy grass–specific IgG_4 increased in response to both SCIT and SLIT over the first 2 years of the trial compared to placebo, with SCIT inducing a higher level of IgG_4 compared to SLIT (Fig 6, *C*). In contrast, SLIT induced a higher level of IgA compared to SCIT. Previous studies have shown that IgE level correlated with frequency of T_H2A cells.[17,18] Here we found that the grass-specific IgE levels positively correlated with frequency of Phl p–specific $CRTH2^{hi}CD27^{lo}$ cells and total Phl p–specific cells for the entire cohort throughout the study (Fig 6, *D*), whereas the IgG_4 levels only correlated with frequency of Phl p–specific $CRTH2^{hi}CD27^{lo}$ cells and total Phl p–specific $CD4^+$ T cells for the SCIT and SLIT groups and not with the placebo group (Fig 6, *D*). No correlation between timothy grass–specific IgA and frequency of Phl p–specific T cells was observed (Fig 6, *D*).

DISCUSSION

We examined the heterogeneity of allergen-specific $CD4^+$ T cells with CyTOF and used unsupervised clustering to examine the phenotype of Phl p–specific cells. The phenotype of these cells can be categorized into two major metaclusters: a $CRTH2^{hi}CD27^{lo}$ metacluster and a $CRTH2^{lo}CD27^{hi}$ metacluster.

Cells within the $CRTH2^{lo}CD27^{hi}$ metacluster represent distinct subsets of T helper cells, including naive/T_H1 cells and conventional $CCR4^+CRTH2^-$ T_H2 cells. Notably, all cells in the $CRTH2^{lo}CD27^{hi}$ metacluster, with the exception of cells in cluster 1, are $CD161^-$.

Cells within the $CRTH2^{hi}CD27^{lo}$ metacluster exhibited the classic T_H2A markers (ie, $CRTH2^+CD49d^+CD27^-$) and produced higher levels of T_H2 cytokines. We speculate that the different clusters within the $CRTH2^{hi}CD27^{lo}$ metacluster represent a mix of T_H2A cells at various stages of development or activation. These T_H2A cells are likely differentiated from the $CD161^+CRTH2^{lo}CD27^+$ T_H2 subpopulation (cluster 1) within the $CRTH2^{lo}CD27^{hi}$ metacluster, as this is the only subpopulation within the $CRTH2^{lo}CD27^{hi}$ metacluster that is $CD161^+$, a marker for T_H2A cells.

For T_H2A cell ontogeny, we propose a model in which $CD27^+CD25^-CD127^-CD161^+CRTH2^-$ T_H2 cells (cluster 1) act as progenitors for T_H2A cells. On early allergen exposure, these progenitors transition into the $CD27^+CD25^-CD127^-CD161^+CRTH2^+$ subset (cluster 7). The basis for this hypothesis is that T_H2A cells are derived from conventional T_H2 cells,[3,6] and cells in clusters 1 and 7 have very similar surface phenotypes. On further stimulation by allergen, cells in cluster 7 upregulate CD25, CD127, and CD161 and transit into the cluster 5 state, which attains the full surface phenotype of T_H2A cells (ie, $CD25^+CD127^+CD161^+CRTH2^+CD39^+$). This scenario is supported by the pseudotime pathway analysis (Fig E3).

A $CCR4^-$ and a $CD161^-$ T_H2A subset were also observed in the $CRTH2^{hi}CD27^{lo}$ metacluster, these may be subsets of cells that have lost expression of CCR4 or CD161 during T_H2A cell differentiation or differentiate directly from a $CD27^{hi}$ subset. In either case, cells from both of these $CCR4^-$ and $CD161^-$ subsets are likely trafficking to other tissues compared to the $CCR4^+$ and $CD161^+$ counterpart. Pizzarello et al also reported the presence of a $CRTH2^{hi}CD27^{lo}$ $CD161^-$ population in infants, which is associated with atopic dermatitis and food allergy.[19] They reported that this $CD161^-$ population was elevated before the elevation of the $CD161^+$ population in infants that developed allergy, and they postulated that $CD161^-$ may be a precursor of T_H2A cells.

We speculate that a robust expansion of $CRTH2^{lo}CD27^{hi}$ cells under a suitable milieu is essential for the development of T_H2A cells from T_H2 cells. We observed that Phl p 1–specific cells have a higher proportion of the $CRTH2^{hi}$ population compared to Phl p 5b–specific cells. This observation suggests that Phl p 1–specific T cells are more capable of undergoing extensive proliferation and differentiation on allergen exposure, whereas Phl p 5b–specific T cells do not exhibit the same capacity. Higher frequencies of Phl p 1–specific cells compared to Phl p 5–specific cells were indeed observed in other studies.[20] This difference in degree of expansion of different Phl p–specific cells may be due to antigen load or antigen processing, leading to a higher abundance of MHC class II/Phl p 1 complexes compared to MHC class II/Phl p 5b complexes.

An earlier study shows that SLIT and SCIT differentially modulate allergen-specific T cells. In that study, although both allergen immunotherapies elicit IL-10 responses, a decrease in IL-5 was only observed in the SCIT group.[21] The current study also examined the effect of SLIT and SCIT on allergen-specific $CD4^+$ T cells. SCIT preferentially depleted cells in the T_H2A-like $CRTH2^{hi}CD27^{lo}$ metacluster. In contrast, SLIT preferentially depleted the $CRTH2^{lo}CD27^{hi}$ subset, which consists of classical T_H2 cells. Frequencies of allergen-specific in both subsets show positive correlation with TNSS scores. As a consequence, decreased frequencies of $CRTH2^{lo}$ and $CRTH2^{hi}$ cells were correlated with improved TNSS of participants receiving SLIT or SCIT, respectively, for both years 1 and 2, similar to what was observed with multimer assays in the GRASS trial.[11] Despite a rebound worsening of TNSS after discontinuation of SCIT or SLIT, neither $CRTH2^{lo}$ nor $CRTH2^{hi}$ cells changed significantly after therapy was discontinued. This observation contrasts with what was observed with multimer assays in the GRASS trial, wherein $CRTH2^{hi}$ cells increased after therapy discontinuation.[11] Reasons for this discrepancy include different experimental approaches and a different set of samples from the previous study. The use of a more comprehensive panel of multimers and a larger sample size may provide a stronger correlation. We also cannot discount the possibility that frequencies of nasal-resident Phl p–specific T cells rather than those in peripheral blood are a better biomarker for monitoring clinical symptoms.

In addition to the differential effects of SLIT and SCIT on allergen-specific T cells, these two delivery approaches also have distinct effects on allergen-specific IgG_4 and IgA.[11,22] SLIT induces higher levels of IgA compared to SCIT, while SCIT induces higher levels of IgG_4. We examined the correlation between allergen-specific T-cell frequencies and IgA and IgG_4 levels.

Our data showed a weak correlation between serum IgG_4 levels and the frequency of $CRTH2^{hi}CD27^{lo}$ cells, but not with frequency of $CRTH2^{lo}CD27^{hi}$ cells. In contrast, IgA levels did not correlate with frequency of either the $CRTH2^{hi}$ or $CRTH2^{lo}$ metaclusters or total Phl p–specific cells. The differential effects of SLIT and SCIT on T cells, IgG_4, and IgA observed are likely due to differences in (1) the allergen dose used—Grazax (75,000 SQ-T/mL) for SLIT versus Alutard SQ Grass Pollen (100,000 SQ-U/mL) for SCIT; (2) the allergen uptake sites (submandibular lymph nodes for SLIT vs axillary lymph nodes for SCIT); and (3) the frequency of repeated exposure (daily for SLIT vs monthly for SCIT during the maintenance phase).

Previous findings have shown that $CRTH2^+$ T_H2A cells produce more T_H2 cytokines and are directly correlated with serum IgE level, whereas $CRTH2^{lo}$ cells produce IFN-γ and IL-10.[3,17,20] Consistent with this, we found that cells within the $CRTH2^{hi}$ subset exhibit higher activation and higher T_H2 cytokine production, whereas cells within the $CRTH2^{lo}$ subset produce higher levels of IFN-γ. Low levels of TGF-β and IL-10 were detected in both populations of T cells, with no significant difference between them. Because TGF-β and IL-10 promote regulatory T-cell differentiation and IgA class switching,[23-25] a reduction in allergen-specific cells in both groups could theoretically result in lower IgA levels after antigen immunotherapy. However, the observed increase in IgA after immunotherapy, particularly after SLIT, suggests that monocytes, macrophages, and regulatory B and T cells rather than allergen-specific effector T cells are the dominant source of these cytokines. Together, the preferential reduction of $CRTH2^{hi}$ and $CRTH2^{lo}$ antigen-specific cells through SCIT and SLIT, coupled with distinct IgG_4 and IgA responses, suggest that quantitative differences and relative balance in T_H1, T_H2, and immunoregulatory cytokines shape both B-cell class switching and T-cell differentiation within local immune environments elicited by these two forms of immunotherapy.

The current study is limited by the relatively small numbers of people enrolled onto the current cohort. Further experiments with other cohorts and use of single-cell RNA sequencing to examine allergen-specific cells in longitudinal samples should validate the current findings and provide further insights into the different pathways invoked by SLIT and SCIT in induction of tolerance.

DISCLOSURE STATEMENT

Supported by the National Institute of Allergy and Infectious Diseases of the National Institutes of Health (NIH) under Award UM1AI09565 and R01 AI095074. This report is the result of funding in whole or in part by the NIH. It is subject to the NIH Public Access Policy. Through acceptance of this federal funding, NIH has been given a right to make this report publicly available in PubMed Central upon the Official Date of Publication, as defined by NIH.

Disclosure of potential conflict of interest: The authors declare that they have no relevant conflicts of interest.

We acknowledge the GRASS study team and the GRASS study participants. We also acknowledge the Benaroya Research Institute (BRI) Center for Interventional Immunology and BRI Clinical Core Laboratory for PBMC collection and processing, the BRI Human Immunophenotyping Core for mass cytometry, and the BRI Protein and Tetramer Core for HLA-II tetramers. We also thank the M. J. Murdock Charitable Trust for generously providing equipment funding for the BRI Cores.

Key messages

- **SCIT depletes $CRTH2^{hi}CD27^{lo}$ T_H2A cells.**
- **SLIT depletes $CRTH2^{lo}CD27^{hi}$ T_H2 cells.**
- **TNSS and both timothy grass–specific IgG_4 and IgE serum levels, but not IgA level, are correlated with frequency of Phl p–specific T cells.**

REFERENCES

1. Savoure M, Bousquet J, Jaakkola JJK, Jaakkola MS, Jacquemin B, Nadif R. Worldwide prevalence of rhinitis in adults: a review of definitions and temporal evolution. Clin Transl Allergy 2022;12:e12130.
2. Bonvalet M, Moussu H, Wambre E, Ricarte C, Horiot S, Rimaniol AC, et al. Allergen-specific $CD4^+$ T cell responses in peripheral blood do not predict the early onset of clinical efficacy during grass pollen sublingual immunotherapy. Clin Exp Allergy 2012;42:1745-55.
3. Wambre E, Bajzik V, DeLong JH, O'Brien K, Nguyen QA, Speake C, et al. A phenotypically and functionally distinct human T_H2 cell subpopulation is associated with allergic disorders. Sci Transl Med 2017;9:eaam9171.
4. Suhrkamp I, Scheffold A, Heine G. T-cell subsets in allergy and tolerance induction. Eur J Immunol 2023;53:e2249983.
5. Gomez RA, Hou J, Gersuk VH, Chow IT, Farrington ML, Robinson D, et al. Ara h $2_{105-124}$–specific T_H2A cells drive peanut allergy in DRB1*15:01 individuals: a detailed epitope analysis. Clin Exp Allergy 2025;55:820-33.
6. Huang Z, Chu M, Chen X, Wang Z, Jiang L, Ma Y, et al. T_H2A cells: the pathogenic players in allergic diseases. Front Immunol 2022;13:916778.
7. Passalacqua G, Canonica GW. Allergen immunotherapy: history and future developments. Immunol Allergy Clin North Am 2016;36:1-12.
8. Tankersley M, Winders T, Aagren M, Brandi H, Pedersen MH, Loftager ASL, et al. Subcutaneous immunotherapy takes more than the time in the clinic. Curr Med Res Opin 2021;37:1925-31.
9. Passalacqua G, Bagnasco D, Canonica GW. 30 years of sublingual immunotherapy. Allergy 2020;75:1107-20.
10. Scadding GW, Calderon MA, Shamji MH, Eifan AO, Penagos M, Dumitru F, et al. Effect of 2 years of treatment with sublingual grass pollen immunotherapy on nasal response to allergen challenge at 3 years among patients with moderate to severe seasonal allergic rhinitis: the GRASS randomized clinical trial. JAMA 2017;317:615-25.
11. Renand A, Shamji MH, Harris KM, Qin T, Wambre E, Scadding GW, et al. Synchronous immune alterations mirror clinical response during allergen immunotherapy. J Allergy Clin Immunol 2018;141:1750-60.e1.
12. Uchtenhagen H, Rims C, Blahnik G, Chow IT, Kwok WW, Buckner JH, et al. Efficient ex vivo analysis of $CD4^+$ T-cell responses using combinatorial HLA class II tetramer staining. Nat Commun 2016;7:12614.
13. Leong ML, Newell EW. Multiplexed peptide-MHC tetramer staining with mass cytometry. Methods Mol Biol 2015;1346:115-31.
14. DeGottardi Q, Gates TJ, Yang J, James EA, Malhotra U, Chow IT, et al. Ontogeny of different subsets of yellow fever virus–specific circulatory $CXCR5^+$ $CD4^+$ T cells after yellow fever vaccination. Sci Rep 2020;10:15686.
15. Ellis B, Haaland P, Hahne F, Le Meur N, Gopalakrishnan N, Spidlen J, et al. flowCore: basic structures for flow cytometry data. R package v2.23.2 2026. Available at: https://bioconductor.org/packages/flowCore.
16. Trapnell C, Cacchiarelli D, Grimsby J, Pokharel P, Li S, Morse M, et al. The dynamics and regulators of cell fate decisions are revealed by pseudotemporal ordering of single cells. Nat Biotechnol 2014;32:381-6.
17. Renand A, Archila LD, McGinty J, Wambre E, Robinson D, Hales BJ, et al. Chronic cat allergen exposure induces a T_H2 cell–dependent IgG_4 response related to low sensitization. J Allergy Clin Immunol 2015;136:1627-35.e1-13.
18. Calise J, DeBerg H, Garabatos N, Khosa S, Bajzik V, Calderon LB, et al. Distinct trajectories distinguish antigen-specific T cells in peanut-allergic individuals undergoing oral immunotherapy. J Allergy Clin Immunol 2023;152:155-66.e9.
19. Pizzarello CR, Jackson CM, Herman K, Seppo AE, Rebhahn J, Scherzi T, et al. A phenotypically distinct human T_H2 cell subpopulation is associated with development of allergic disorders in infancy. Allergy 2025;80:949-64.
20. Wambre E, Delong JH, James EA, Torres-Chinn N, Pfutzner W, Mobs C, et al. Specific immunotherapy modifies allergen-specific $CD4^+$ T-cell responses in an epitope-dependent manner. J Allergy Clin Immunol 2014;133:872-9.
21. Schulten V, Tripple V, Aasbjerg K, Backer V, Lund G, Wurtzen PA, et al. Distinct modulation of allergic T cell responses by subcutaneous vs sublingual allergen-specific immunotherapy. Clin Exp Allergy 2016;46:439-48.

22. Shamji MH, Larson D, Eifan A, Scadding GW, Qin T, Lawson K, et al. Differential induction of allergen-specific IgA responses following timothy grass subcutaneous and sublingual immunotherapy. J Allergy Clin Immunol 2021;148:1061-71.e11.
23. van de Veen W. The role of regulatory B cells in allergen immunotherapy. Curr Opin Allergy Clin Immunol 2017;17:447-52.
24. Boonpiyathad T, Satitsuksanoa P, Akdis M, Akdis CA. IL-10 producing T and B cells in allergy. Semin Immunol 2019;44:101326.
25. Celebi Sozener Z, Mungan D, Cevhertas L, Ogulur I, Akdis M, Akdis C. Tolerance mechanisms in allergen immunotherapy. Curr Opin Allergy Clin Immunol 2020; 20:591-601.